Evaluating Human Electromagnetic Exposure in a Unmanned Aerial Vehicle (UAV)-aided Network

Thomas Detemmerman

Supervisor(s): Prof. dr. ir. Wout Joseph, Prof. dr. ir. Luc Martens

Abstract—Society relies more than ever on the availability of wireless networks. Due to the mobility of a UAV, a UAV-aided network is able to provide this necessary access in case the existing terrestrial network gets damaged. However, the public is concerned about the potential health effects of the electromagnetic radiation caused by these networks. Therefore, mobile devices and base stations have to comply to strict legislation enforced by the government.

This research investigates how different scenarios influence power consumption, electromagnetic exposure and specific absorption rate. These different scenarios are defined by various flying heights, number of UAVs available and population densities. Further, also an analysis on the difference between a realistic microstrip patch antenna and a fictional equivalent isotropic radiator is performed. Thereafter, the network will be optimized towards goals like electromagnetic exposure of the average user or power consumption of the entire network; which results in conflicting requirements.

To accomplish this goal, a capacity based deployment tool will be used which simulates an entire UAV-aided network. In this way, all important sources for electromagnetic radiation, like all user equipment and all flying base stations, will be considered.

It looks from the results that a power consumption optimized network with a fixed flying height of 80 metres is the recommended approach for the city centre of Ghent. A microstrip patch antenna with a sufficiently large aperture angle is a good starting point. However, different antenna array configurations still have to be investigated.

Keywords— deployment tool, electromagnetic exposure, LTE microstrip patch antenna, power consumption, radiation pattern, specific absorption rate (SAR), UAV, unmanned aerial base stations

I. Introduction

SOCIETY is constantly getting more and more dependent on wireless communication. On any given moment, in any given location, an electronic device can request to connect to the bigger network, starting from small Internet of Things (IoT) up to self-driving cars.

Also in exceptional and possibly life threatening situations, the public relies on the cellular network despite the fact that the network might be severely damaged and not properly functioning anymore. One solution for a fast temporarily deployable back-up network is to use UAVs. A base station can be attached to these flying UAVs to support the network over a limited area. This approach is also useful in case of an unexpected increase in traffic. For example during the terrorist attacks at Brussels Airport, mobile network operators saw all telecommunications drastically increasing causing moments of contention. Some operators even decided to temporarily exceed the exposure limits in order to handle all connections [1]. Electromagnetic exposure caused by these networks can however not be neglected. Research shows how excessive electromagnetic radiation can cause diverse biological side effects [2], [3]. It becomes clear that electromagnetic exposure is a key value when designing a UAV-aided network and should definitely not surpass the limits predefined by the government.

UAV-aided networks can, thanks to their mobility, easily be repositioned towards a certain goal. Several papers explain how a network can be optimized towards different goals like power consumption. However, very limited research has been done where a UAV-aided network is optimized towards electromagnetic exposure. While several publications exist, discussing how the electromagnetic exposure can be calculated, most of them only consider a limited number of sources; e.g. only base stations or only the user's mobile device. Papers who cover electromagnetic exposure from all the different sources and convert it into a single value are rather limited.

This research proposes a method to optimize the network towards electromagnetic exposure and power consumption when considering all four sources of radiation in a telecommunications network, being: the user's own phone, the base station that is serving this user, all devices from other users in the network and all other active base stations that are not serving this user. In this way, the contribution of each source towards the total electromagnetic exposure can easily be identified.

The behaviour of the electromagnetic exposure and power consumption of the network will be analysed by applying the tool in different scenarios by using different types of antennae, various flying height and population densities. Values like Specific Absorption Rate (SAR), electromagnetic exposure and power consumption will give insight in how the network behaves so the network could be optimized accordingly.

To make this research possible, an existing capacity based deployment tool developed by the WAVES research group at Ghent University is extended for the specific purpose. This planning tool describes a fully configured UAV-network which is a suitable starting point for this research.

II. State of the Art

A. Electromagnetic exposure

Users in a telecommunication network are exposed to various sources of electromagnetic radiation, expressed in V/m. Once the exposure is absorbed by the human body, we speak of the specific absorption rate (SAR) which is expressed in W/kg. All these values are subjected to limitations enforced by the government. This research is based in Ghent, a Flemish city in Belgium where the 2.6 GHz frequency band, an individual antenna cannot exceed 4.5 V/m and the cumulative sum of all fixed sources has its

maximum at 31 V/m [4], [5]. The maximum whole body SAR-values for a mobile device over a 10 g tissue (SAR_{10g}) is defined at $2W/kg$ [6].

Several papers calculate exposure originating from specific sources [7], [8], [9], [10] where some convert the uplink (UL) radiation into localized specific absorption rates [9], [10]. With the advent of 5G, paper [11] describes how the localized SAR-values are achieved from all different sources. Finally, [12] describes how the electronic radiation can be converted into whole body SAR values.

In a realistic network, some users are calling while others are using other types of telecommunication services like browsing the web. Therefore, all absorbed electromagnetic exposure should be expressed in whole body SAR while still covering all sources.

B. Optimized UAV-aided networks

A UAV knows several applications. It was originally mainly used to support the military for surveillance and remote attacks without endangering pilots [13]. However, UAVs have recently become more accessible by the general public due to decreasing costs. This allowed UAVs to be researched for various applications.

A UAV equipped with a femtocell base station antenna is called a Unmanned Arial Base Station (UABS) which brings several advantages like mobility and rapid deployment. However, it brings also challenges like limited weight of the payload and sparse power supply.

Kawamoto et al. introduced in [14] a WiFi network with the support of UAVs while considering resource allocation and antenna directivity. Gangula et al. illustrates in [15] how UAVs can be used as a relay for Long-Term Evolution (LTE) and Zeng et al. proposes in [13] a tutorial in 5G-and-beyond wireless systems where challenges like energy consumption, mobility and antenna direction are discussed. In [16], Deruyck et al. designed a capacity based deployment tool for UAV-aided emergency networks for large-scale disaster scenarios where an ideal flying height of 100 m is suggested. This was expanded in [17] with a performance evaluation of the direct-link backhaul of this tool where a slightly lower flying height of 80 metres is recommended.

Mozaffari et al. provides in [18] guidelines on how to optimize and analyse UAVs equipped for wireless communication equipment. A research area that has been excessively studied is the location solution optimization problem where networks are designed in such a way that certain goals like minimal power consumption or shortest flying distance are achieved [19], [20], [21], [22]. These optimizations can be done through different implementation methods like exact algorithms or machine learning [18], [23].

Research where network is optimized towards electromagnetic exposure is rather limited. Deruyck et al. discusses in [8] how a terrestrial network can be optimized towards either a minimal exposure or minimal power consumption of the entire network. However, to the best of the author knowledge, no research has been done where a UABS-network has been optimized towards electromagnetic exposure.

C. Technologies

For the deployment of the network, the more robust UAV from [16] will be used (details in table II) and will be operating in the 2.6 GHz bandwidth. Since the users are assumed to experience a constant electromagnetic exposure without interruptions, frequency division duplex is used.

The onboard antenna of the UAV will act as the gateway between the UE and the backhaul network. However, determining which antenna to use and how to position it, can be challenging. The radiation pattern from the antenna can be influenced by the UAV [24]. Also the fact that the UAV will hover above the user makes tradional 2D modelling insufficient. A 3D-model which accounts for both elevation and azimuth directivity will be required [13].

The easiest radiation pattern is a hypothetical isotropic radiator which radiates equally in all directions. Antennae that radiate equal quantities for a certain plane are called omnidirectional antennae [13] and several UABSs use antennae like monopoles, dipoles and wing antennae [25], [26], [27], [28]. Another type of antennae are directional antennae which save energy by focussing the electromagnetic energy where it is needed. One type that has excessively been researched in various array-configurations is a microstrip patch antenna [29], [30], [31]. These provide several advantages compared to traditional antennae [32], [33] like lightweightness, low in cost causing them to be more aerodynamic.

A basic microstrip antenna consists of a ground plane and a radiating patch, both separated by a dielectric substrate. Several variations exist like microstrip patch antennae, microstrip slot antennae and printed dipole antennae which all have similar characteristics [32], [33]. They all are thin, support dual frequency operation and they all have the disadvantage that they will transmit at frequencies outside the aimed band which is also known as spurious radiation. The microstrip patch and slot antenna support both linear and circular polarization while the printed dipole only supports linear polarization. Further, the fabrication of a microstrip patch antenna is considered to be the easiest of the considered patch antennae [32].

Figure 1 shows a microstrip patch antenna constructed out of an aluminium patch and a teflon substrate. The microstrip patch antenna is pointing towards the ground since the UAV will be flying above the user.

III. Methodology

A. Electromagnetic Exposure

A.1 Total Electromagnetic Exposure

The total whole body SAR ($SAR_{10g}^{wb,total}$) of a user can be calculated by a simple sum of individual SAR values from the different sources and is based on [11]. This formula assumes that the users are holding their device next to their ear and therefore investigates localized SAR for head and torso area. However for this case, this would result into incorrect conclusions since the position of the device relative to the user is unknown. The position of the phone can

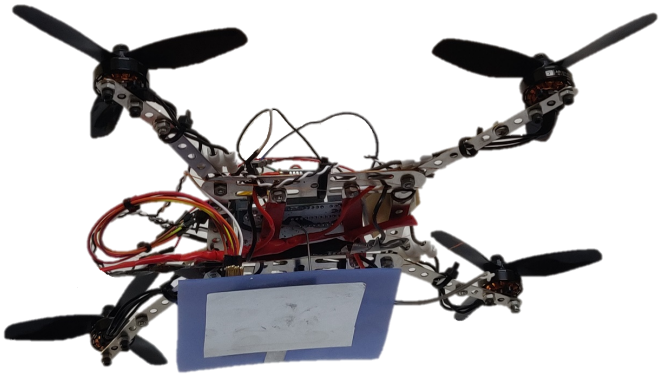

Fig. 1: Image of a microstrip patch antenna attached to the bottom of a UAV.

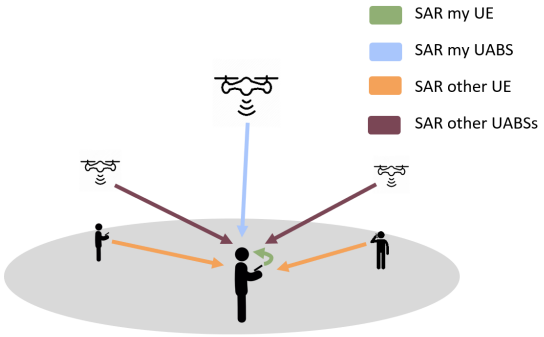

Fig. 2: Illustration of the network that shows how the average user (here shown in the center) is influenced by different types of sources.

be next to the head but also in front of the user. The induced electromagnetic radiation will therefore be expressed in function of the entire body.

$$SAR_{10g}^{wb,total} = SAR_{10g}^{wb,myUE} + SAR_{10g}^{wb,myUABS} + SAR_{10g}^{wb,otherUE} + SAR_{10g}^{wb,otherUABSs} \quad (1)$$

The first parameter, $SAR_{10g}^{wb,myUE}$, indicates the absorbed electromagnetic radiation by the whole body originating from the user's own device. Despite that the UL radiation is destined for the serving UABS, a portion of that radiation is directly absorbed by its user, due to the omnidirectional nature of the mobile's antenna. The second parameter, $SAR_{10g}^{wb,myUABS}$, represents the downlink (DL) radiation caused by the UABS that is serving the user. As the third parameter, we have the $SAR_{10g}^{wb,otherUE}$ which is radiation caused by other people's devices. The radiation of these devices is once again destined for a specific UABS but again, a portion of that UL radiation will also be absorbed by our user. Finally, $SAR_{10g}^{wb,otherUABSs}$ represents the DL radiation by the other UABSs to which our user is exposed to but not served by. An illustration is given in figure 2. The green arrow stands for near-field radiation, the others represent far-field radiation.

A.2 Electromagnetic Radiation from a Single Source

Calculating far-field exposure in a certain point needs to be done for all UABSs and UE, except for the device present in that specific point which will be near-field radiation and has to be calculated differently. The exposure E of a single user u from a single radiator i can be calculated as follows.

$$E_i(u)[V/m] = 10^{\frac{RRP(u)[dBm]-43.15+20*\log(f[MHz])-PL(u)[dB]}{20}} \quad (2)$$

Calculating the real radiation power (RRP) for a certain user u, requires first the equivalent isotropic radiation power (EIRP)-value to be calculated [7], [8]. This is achieved by adding the transmission power P_{tx} to the transmitter gain G_t and thereafter subtracting the feeder loss L_t. This formula needs to be expanded to also account for attenuation from the used antenna. This value depends on the angle between this user and the antenna's main beam. The attenuation from an equivalent isotropic radiator is always zero. This leads to the following formula.

$$RRP[dBm] = P_{tx}[dBm] + G_t[dBi] - L_t[dB] - attenuation(u)[dB] \quad (3)$$

The used frequency in formula 2 is denoted as f and is expressed in MHz. Since LTE is used, this value will be 2600 MHz.

At last, formula 2 requires the path loss PL. In order to calculate this, an appropriate propagation model — of which several exist— is required. The Walfish-Ikegami model is used since it performs well for femtocell networks in urban areas [16].

A.3 Combining Exposure

The total electromagnetic exposure E_{tot}, in a certain spot, originating from different sources can be calculated with formula 4. E_i stands for the electromagnetic exposure from source i and n stands for all far-field radiators of a certain category which will either be UABSs or UE from other people. E_{tot} will be calculated for each location where a user is positioned.

$$E_{tot}[V/m] = \sqrt{\sum_{i=1}^{n}(E_i[V/m])^2} \quad (4)$$

A.4 Converting electromagnetic radiation into SAR-values

Formula 1 expects that the radiation is expressed in whole body SAR-values. To make this calculation possible, a distinction has to be made between near-field SAR ($SAR^{wb,nf}$) and far-field SAR ($SAR^{wb,ff}$). $SAR_{10g}^{wb,myUABS}$ is a form of near-field radiation, all the other types are far-field radiation.

Converting the electromagnetic radiation is done with a conversion factor which is based on Duke of the Virtual

Family. Duke is a 34-year old male with a weight of 72 kg, a height of 1.74 m and body mass index of 23.1 kg/m [12]. Research shows that the conversion factor for WiFi in the far-field is $0.0028\frac{W/kg}{W/m^2}$ and $0.0070\ \frac{W/kg}{W}$ for the near-field [12]. Since WiFi, at a frequency of 2400 MHz, is very close to LTE, at 2600 MHz, it is assumed in [12] that this value is also applicable for LTE. Calculating SAR from far-field radiation is done as follows.

$$S[W/m^2] = \frac{(E_{tot}[V/m])^2}{337} \tag{5}$$

$$SAR_{10g}^{wb,ff}[W/kg] = S[W/m^2] * 0.0028 \left[\frac{W/kg}{W/m^2}\right] \tag{6}$$

The constant in equation 6 converts the power flux density S to the required $SAR_{10g}^{ff,wb}$. To make this possible, the electromagnetic radiation from formula 4 should first be converted to the power flux density with formula 5.

The SAR caused by near-field radiation is calculated by multiplying the constant with the used transmission power P_{tx} of the User Equipment (UE) which results to the following formula.

$$SAR_{10g}^{wb,nf}\left[\frac{W}{kg}\right] = 0.0070\left[\frac{W/kg}{W}\right] * P_{tx}[W] \tag{7}$$

B. Microstrip Patch antenna

A microstrip patch antenna is chosen because it allows easy production but more important, it has a low weight and has a thin profile causing it to be very aerodynamic which is useful when attaching it to a drone [32].

The dimensions of the antenna depend on the frequency it is operating at and the characteristics of the used substrate. The antenna will be radiating at a centre frequency f_0 of 2.6 GHz. Each substrate has a dielectric constant ϵ_r representing the permittivity of the substrate that depends on the used material. Substrates with a high dielectric constant and low height reduce the dimensions of the antenna while a lower dielectric constant with a high height improves the performance of the antenna [33], [34]. In this research, a substrate like glass is chosen because of the higher dielectric constant of $\epsilon_r = 4.4$ compared to materials like Teflon with only a dielectric constant of $\epsilon_r = 2.2$ [33]. Doing this in combination with an antenna height of 2.87 mm will decrease the dimensions of the entire antenna surface. This comes in handy since drones only have limited space available.

description	symbol	value
centre frequency	f_0	2600 Hz
dielectric constant	ϵ_r	4.4
height of the substrate	h	0.00287 m

TABLE I: Overview of configuration parameters.

The dimensions of the radiating patch can be calculated with the formulas from [33], [34]. Doing so will result in a radiating patch of 35.09 mm by 26.55 mm and a groundplane of at least 52.40 mm by 43.80 mm. The microstrip patch antenna as illustrated in fig. 3 will result in the radiation pattern of fig. 5.

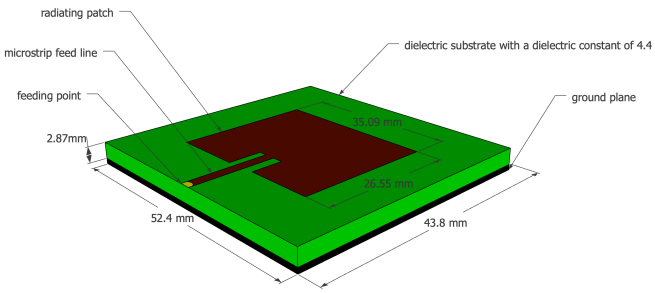

Fig. 3: Design of the microstrip patch antenna.

C. Optimizing the network

Deruyck et al. discusses in [8] how a terrestrial telecommunication network either can be optimized towards electromagnetic exposure of an individual or towards power consumption of the entire network. However, an increasing transmission power of an antenna comes with an increasing electromagnetic exposure. This is not the case considering both values for an entire network. In fact, the authors from [8] prove that both become inversely equivalent. The reason why the network behaves like this is because it is often cheaper to increase the exposure of an already active base station than activating a new one. This leads to the following fitness function which is based on [8].

$$f = w * \left(1 - \frac{E_m}{E_{max}}\right) + (1 - w) * \left(1 - \frac{P}{P_{max}}\right) * 100 \tag{8}$$

Formula 8 returns a fitness value which represents the performance of the entire network. w is the importance factor of electromagnetic exposure ranging from 0 to 1, boundaries included. A w set to 0 means that electromagnetic exposure is not important. Such network will therefore be called a power consuption optimized (PwrC. Opt.) network. Likewise, a w set to 1 means that minimizing exposure is top priority and will result in an exposure optimized (Exp. Opt.) network. P_{max} is the power consumption of all UABSs, both active and inactive, when radiating at the highest level possible while P is the effective power used by the current designed network. This will be the power required for the flying drones themselves and their antennae. E_m will be the weighted exposure of the average user for the current designed network and E_{max} the weighted average of the electromagnetic exposure when all antennae are at their highest power level.

When optimizing the network, it is not only important to consider the average exposure of all users, but also to limit high extremes [8]. A weighted average will be used not only considering the median but also the 95 percentile from all users' DL exposure using formula 9. Since both values are considered to have equal importance, the weight factors w_1 and w_2 will both have an equal importance of 50%.

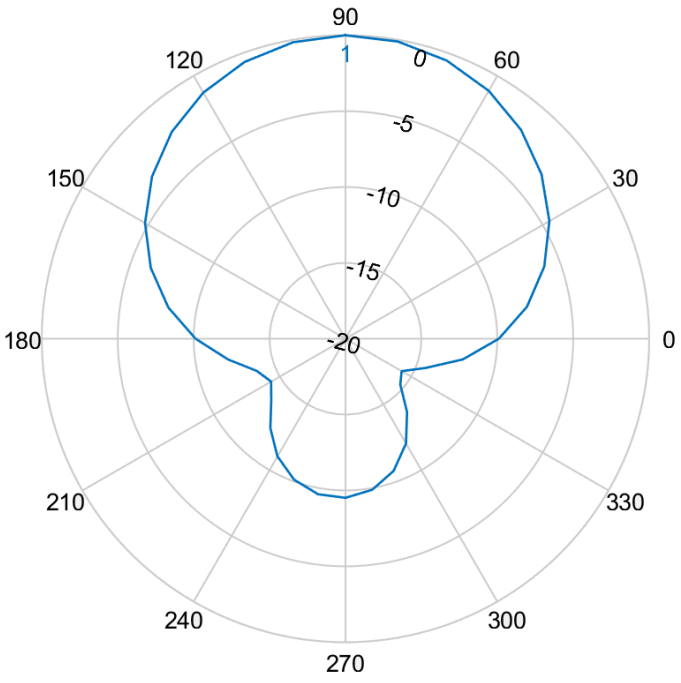

(a) E-plane

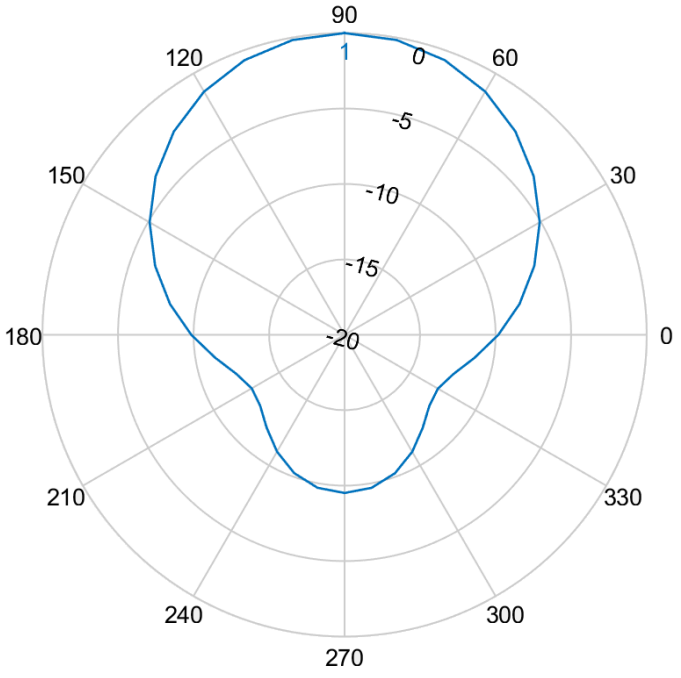

(b) H-plane

Fig. 4: Radiation patterns generated by the used microstrip patch antenna.

$$E_m = \frac{w_1 * E_{50} + w_2 * E_{95}}{w_1 + w_2} \tag{9}$$

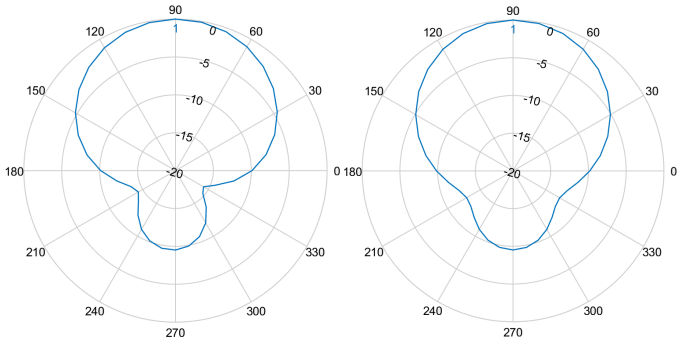

Fig. 5: On the left is the radiation pattern of the E-plane drawn and on the right for the H-plane.

D. Simulation Tool

D.1 Main Algorithm

First, a description of the area has to be provided to the tool. This is done with so-called shape-files. These files contain a complete description about the shape of the buildings. Thereafter, users are uniformly distributed over the area and a temporary UABS is positioned above each user. Now, the decision algorithm needs to decide which of these UABSs can actually remain and how hard each one should be radiating. Once the decision algorithm is done, the tool checks whether the number of online UABSs does not acceed the capacity of the facility where the UABSs are stored. If this is the case, the UABSs covering the least amount of users will be removed.

D.2 Decision Algorithm

Solving the network is done by the decision algorithm and starts by calculating the path loss between all users and between users and UABSs. Thereafter, the algorithm iterates over each user and tries to connect that user to each UABS. This connection is not always possible. A UABS might be saturated with users and will not be able to cover yet another one or maybe the user is so far away that in order to cover that user, the UABS would have to exceed its maximum allowed input power. If however a connection is possible, the user will be connected to that UABS and the fitness function (eq. 8 is applied. This is repeated for each UABS. Only the connection which results in the best fitness value for the entire network will be used. Thereafter, the tool shifts to the next user. When the last user has been processed, the network is fully designed for an unlimited number of drones and the result is returned to the main algorithm for further processing. The flowchart of this algorithm is given in figure 6.

IV. Scenarios

The default configuration is given in table II and is always applicable unless mentioned otherwise.

Three main scenarios will be investigated. The first one has only one user and one UABS present in the network. SAR, electromagnetic exposure, power consumption and

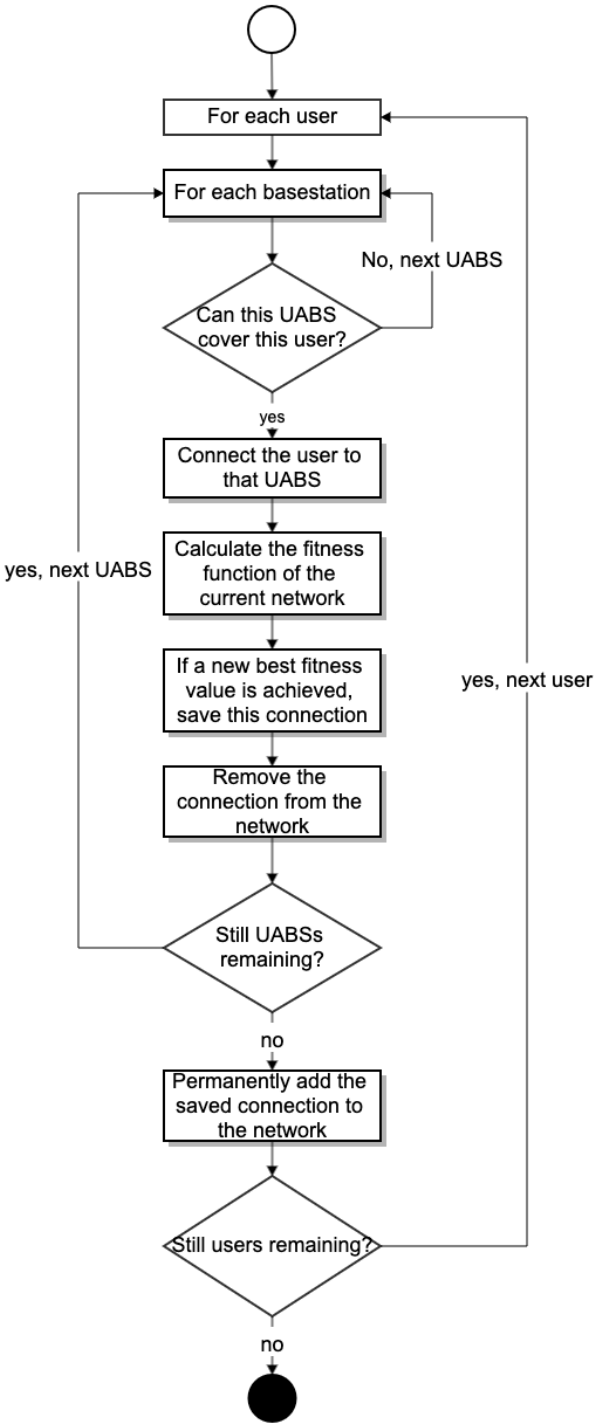

Fig. 6: Flowchart of the decision algorithm.

antenna transmission power are investigated at different flying heights.

In a second scenario, the network is expanded for multiple users while still considering only one UABS. The scenario is divided into two cases. One with a variable flying height but with a fixed number of 224 users as is average on an usual day at 5 p.m. in Ghent [16]. In the other case, the number of users varies but the flying height is set to

Broadband cellular network	
technology	LTE
frequency	2.6 GHz
UAV	
UAV power	13.0 A
average UAV speed	12.0 m/s
average UAV power usage	17.33 Ah
UAV battery voltage	22.2 V
Femtocell antenna	
maximum P_{tx}	33 dBm
antenna direction	downwards (az: 0°; el: 90°)
gain	4 dBm
feeder loss	2 dBm
implementation loss	0 dBm
radiation pattern	EIRP or microstrip patch
flying altitude	100m
UE Antenna	
height	1.5m from the floor
gain	0 dBm
feeder loss	0 dBm
radiation pattern	EIRP
Quantity	224

TABLE II: Overview of default configuration values.

100 metres [16]. The power consumption, electromagnetic exposure and specific absorption rate are investigated for each case.

The third scenario is quite similar to the previous scenario. The same two cases are investigated, but now an unlimited number of UABSs is avalaible.

Each case from each scenario consists out of four possible configurations. There are two possible antennae, namely EIRP and microstrip patch antenna, which can both be applied in a PwrC. Opt. network or an Exp. Opt. network.

It is important to note that all measured values are strictly limited to the sources mentioned in the previous section and thus only cover data traffic between UE and UABSs. Any other potential sources like backhaul links will not be covered. An overview of the simulation configuration scenarios is presented in figure 7

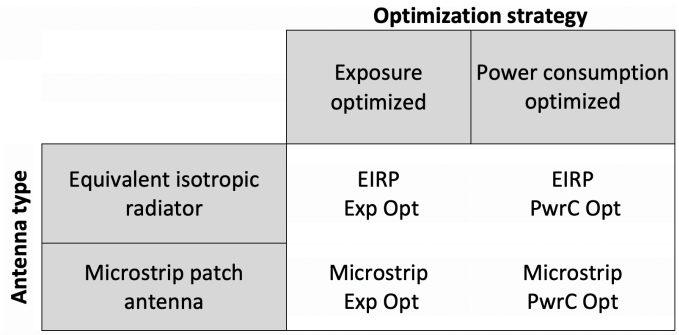

Fig. 7: Matrix with the four possible configurations

V. Results

A. One User and One UAV

The results show that for a varying flying height, a logarithmic relationship exists between the P_{tx} and the flying height. This is mainly caused by the logarithmic scale in which the decibels of the P_{tx} are expressed. So while 10 dBm equals 10 mW, 20 dBm equals 100 mW. Each time the flying height becomes too large to cover, the P_{tx} increases with one dBm. When using the default configuration, with a maximum P_{tx} of 33 dBm, a UABS can fly up to 387 m before losing connection in a free line of sight (LOS) scenario.

This scenario is investigated with a microstrip patch antenna using power consumption optimization. However, the chosen optimization strategy does not really matter because the decision algorithm decides which user needs to be connected to which UABS. Since only one UABS is available, both optimization strategies will behave identical. Further, also the used antenna will not make any difference. The user is namely positioned in the perfect centre of the main beam where there is no attenuation experienced for both antennae.

When investigating this scenario at different flying heights, we notice that the UL radiation increases exponentially while the DL radiation remains constant during the entire time. The reason that the DL radiation remains constant is because of power control which makes sure that no more power is used than strictly necessary. So at lower flying altitudes, there is less path loss and the UABS will therefore reduce the P_{tx}. We can therefore confirm that the electromagnetic exposure is a constant fraction of power and distance. The UL radiation starts very low but surpasses the DL radiation around 80 metres.

B. Increased Population with one UABS

B.1 Variable Flying Height

A PwrC. Opt. network has higher exposure compared to an Exp. Opt. network; a behaviour that was already proven by [8]. However, for this scenario, a PwrC. Opt. network will also result in a higher power consumption. To understand this, the behaviour of the deployment tool needs to be understood first. A PwrC. Opt. network will result in a few high powered UABSs because increasing the input power of an antenna costs less than activating a new UAV. Likewise, an Exp. Opt. network generates a lot of low powered UABSs because the lower the power of the antenna, the lower the exposure. This has the consequence that the cover radius is less and therefore more UAVs, which cost more energy, are required. When only a limited amount of UABSs are available, like only one in this scenario, the tool will only keep UABSs which cover the most users. Therefore, the power consumption in a PwrC. Opt. network is much more higher.

Further, the results also show that the exposure increases with higher flying altitudes because there is a lower probability of having non line of sight (NLOS) links by obstructing buildings. This has as consequence that more users become covered. The increasing electromagnetic radiation is however not unlimited. At even higher flying altitudes, the distance between a given UABS and some users further away becomes too large causing the coverage to decrease again. When this decrease occurs depends on the configuration. A PwrC. Opt. network tends to decline earlier than an Exp. Opt. network.

When replacing the fictional EIRP antenna by a microstrip patch antenna, the percentage of covered users drops for both optimization strategies. This is because users, who have a higher horizontal distance between themselves and the UABS, experience a higher attenuation.

The results further show that the radiation from the UABS is the main factor followed by the near-field radiation from the user's own device. The far-field radiation from other UE barely contributes anything.

B.2 Variable Number of Users

Also the results from this case show how EIRP antennae designs are able to cover more users than microstrip patch antennae just like PwrC. Opt. networks will reach more users than Exp. Opt. networks. The contribution to the total SAR from each individual source is identical to the previous scenario.

There is still only one UABS available. When population grows, more users become uncovered and therefore the average electromagnetic exposure decreases. For example, an EIRP PwrC. Opt. network will have the highest exposure and therefore covers the most users as opposed to a microstrip patch antenna in an Exp. Opt. network which will radiate the least and thus has the lowest number of covered users.

While the population grows, more and more users become uncovered causing the average SAR to drop. However, this does not conclude that by increasing the population, the SAR of a user who is directly beneath a UABS would be less. To investigate this, a user is positioned in the middle of the city centre of Ghent and a UAV is positioned above him. Initially, only 49 people are active around him. The SAR of our central user is monitored while the population around him is growing. Figure 8 shows with the black lines which users are connected. The left map is for only 50 users and shows that only one user is connected besides our central user. The map on the right considers 600 users and shows much more connected users. The results show that the UL SAR of the central user remains constant; a normal behaviour since the flying altitude does not change. The SAR from the UABS experiences a slight increase. When the population grows, more users become available and some will spawn near the central user. The UABS will likely decide to cover these users as well as visible in figure 8. These users might have a slightly worse path loss because of obstructing buildings or a somewhat bigger distance. The UABS reacts to this by increasing its power consumption causing an increase in the DL SAR for the central user. The results further also show that the SAR from other UE increases when the population increases. But as mentioned before, it is much less compared

to the other sources.

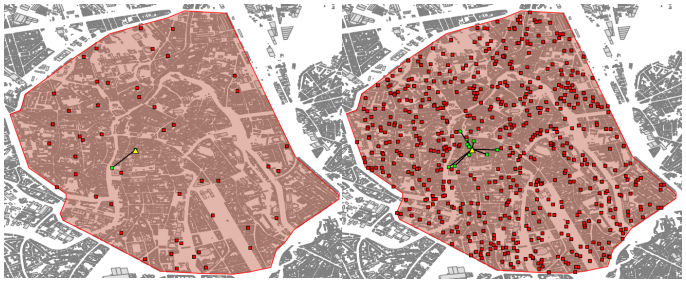

Fig. 8: Overview of which users are connected to the UABS. The map on the left is for 50 active users while the map on the right considers 600 active users.

C. Unlimited Number of UABSs

C.1 Variable Flying Height

The same cases as in the previous scenario are investigated. Only now, an unlimited number of UABSs is available. The results prove that the different optimization strategies work as intended. PwrC. Opt. networks have indeed a lower power consumption but therefore result in higher electromagnetic radiation. On the other hand, an Exp. Opt. network will reduce the electromagnetic exposure by using more UAVs and thence also increase the network's power consumption. This conclusion was already made in [8] and is supported by these results.

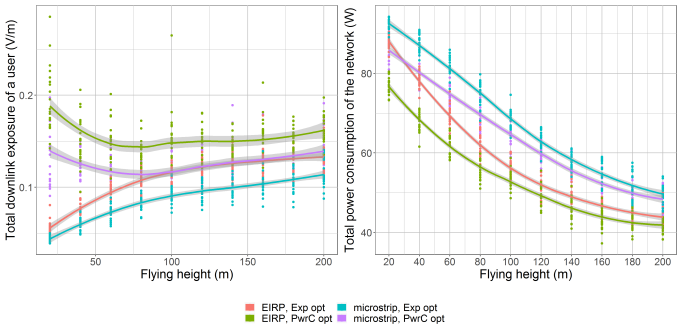

Fig. 9: These two figures show how the flying height influences the downlink electromagnetic radiation of the average user (left) and power consumption of the entire network (right) for an unlimited number of drones.

The exposure in figure 9 shows that an Exp. Opt. network increases logarithmically while the PwrC. Opt. network rather has a concave relationship with the flying height, and has its lowest point at around 70 metres.

At a flying height of 20 m, the Exp. Opt. network has on average 220 to 224 UABSs. That is (almost) one UABS for each user so it is logical that the electromagnetic exposure is very low. The number of UAVs in a PwrC. Opt. network is much less in order to save energy but it is still able to achieve the same percentage of coverage. This is done by increasing the radiation so the cover radius would become larger. The results further show that the network profits from increasing the flying altitude. Not only less UAVs are needed but also the power consumption is lower. Both can be explained by the lower path loss when UABSs fly higher.

Figure 10 shows how each source contributes to the total SAR. A first consequence of higher flying altitudes is the increase in electromagnetic radiation from the user's own device; a behaviour also explained in the first scenario. A second consequence is that also the exposure from 'other UABSs' increases, caused by lower path loss from less obstructing buildings. The figures from 10 further also clearly show that this increase in electromagnetic radiation will be less for a microstrip patch antenna. The reason behind this is that energy will be more focussed towards the ground and there is less sideways radiation because of attenuation.

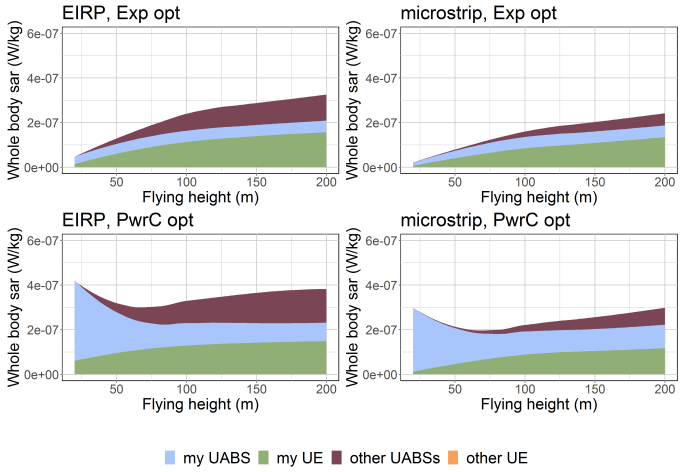

Fig. 10: Each chart corresponds with one of the four possible configurations. The contribution of each source towards the total SAR for a varying flying height is shown.

C.2 Variable Number of Users

When the flying height of the UABSs is fixed to 100 metres and the density of the population increases, also the number of required UAVs increases in order to reach a 100 % coverage. Figure 11 shows that when the number of UABSs and users increases, also the electromagnetic exposure and power consumption increases. Once again, the EIRP antenna in a power consumption network has the highest exposure for the lowest power consumption and a microstrip patch antenna in an Exp. Opt. network the lowest exposure for the highest power consumption. The two other combinations are in the middle and behave very similar.

When looking at the different contributions to the total SAR in figure 12, we see that the weighted average SAR from the users' own device and from the serving UABS remains constant. The flying altitude is always the same so also the required energy to cover that distance will remain the same. The only SAR values that increase are the DL SAR from other UABSs and the UL SAR from other UE. When more users come online, also more UAVs will be radiating. The electromagnetic radiation will thus increase

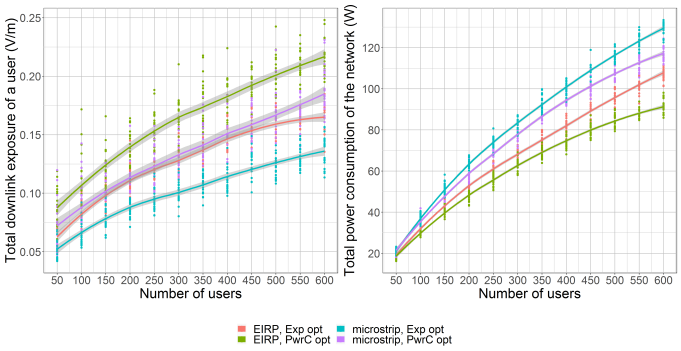

Fig. 11: These two figures show how the number of users influences the downlink electromagnetic radiation of the average user (left) and power consumption of the entire network (right) for an unlimited number of drones.

for both types of sources. Moreover, there is very little path loss at this flying altitude since it is higher than the average building.

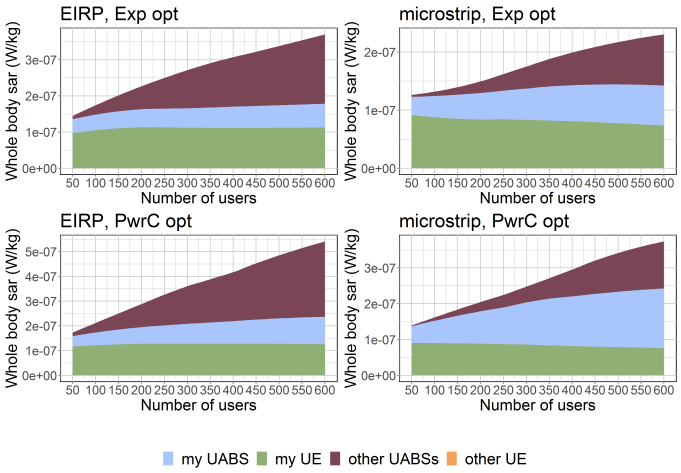

Fig. 12: Each chart corresponds with one of the four possible configurations. The contribution of each source towards the total SAR for a varying number of users shown.

VI. Conclusion

Literature showed that a network can be optimized towards either the power consumption of the entire network or the electromagnetic exposure of the average user using a fitness function [8]. However, the fitness function should be used with care considering that UABSs can be placed anywhere as opposed to the transmission towers from [8] who have a predetermined position. In an Exp. Opt. network, this causes a lot of users to get a UABS all by themselves because this is the best approach to minimize exposure. A PwrC. Opt. network on the other hand will try to limit the number of drones in order to save energy. So as a rule of thumb: an Exp. Opt. network will result in a lot of low powered devices (increasing the overall power consumption) while a PwrC. Opt. network results in a few high powered devices (increasing the exposure of the average user). If the goal is to remain in the air for a longer period of time, an Exp. Opt. network is recommended because the power consumption of an individual UABS is lower. On the other hand, a PwrC. Opt. network is cheaper because less drones are involved. Moreover, the results show that the electromagnetic radiation in a PwrC. Opt. network (with high powered UABSs) is far below the thresholds enforced by the Flemish government.

The user's main sources of exposure are the user's own device and the UABS who is serving him, followed by all other UABSs in the network. When the population increases, there is not only more radiation from UE but also from more UABSs that are serving the other users. The exposure from other people's UE is so low that it can be neglected. An Exp. Opt. network will limit the total exposure mainly by trying to reduce the exposure from other UABSs.

A directional microstrip patch antenna is introduced because it gives several advantages compared to omnidirectional antennae. Directional antennae are able to focus their energy there where it is needed, namely towards the ground. Microstrip patch antennae further benefit from their thin and lightweight design. The performance of this directional microstrip patch antenna has been compared to a fictional equivalent isotropic radiator. This equivalent isotropic radiator has higher exposure and coverage for less power, compared to realistic antennae like microstrip patch antennae because of the absence of attenuation, and can hypothetically be compared with an antenna with a very big aperture angle. This type of antenna can achieve the same coverage with less resources like power and number of drones. A microstrip patch antenna with a more limited aperture angle of 90° requires more resources but causes less sideways radiation. So the exposure from other UABSs will be way less.

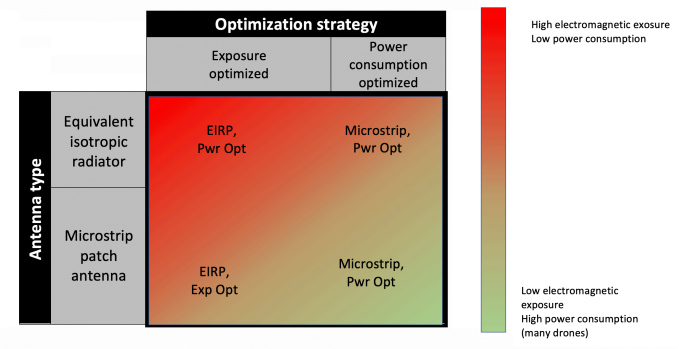

Fig. 13: Matrix with the four possible configurations, colour-coded based on the results.

Remarkable is that an EIRP Exp. Opt. network behaves very similar to a microstrip PwrC. Opt. network as shown in figure 13. This results in the best of both worlds. The microstrip patch antenna will generate less electromagnetic radiation by design and the power consumption optimization reduces the number of required drones and power. A

microstrip patch antenna with an aperture angle of 90° is considered as a good solution but if budget is limited, an antenna with a larger aperture angle would further reduce cost without interfering with the Flemish legislation regarding electromagnetic exposure.

The electromagnetic radiation of an Exp. Opt. network increases with higher flying altitudes. Around 80 metres, the exposure from the user's device surpasses the exposure from the serving UABS. On the other hand, a PwrC. Opt. network shows that the lowest exposure is measured around 70 to 80 metres. Further, the results also show that the number of required drones decreases when the flying height becomes larger; a conclusion that was also made in [16]. When also considering the results from [17] where a flying altitude from 80 metres is suggested for an optimal access and backhaul connectivity, a flying height of 80 metres is also here proposed for the city centre of Ghent.

In short, a PwrC. Opt. network is proposed with a fixed flying height of 80 metres. A microstrip patch antenna with a sufficiently large aperture angle is a good starting point. However, different antenna configurations should be investigated.

Acknowledgement

Special thanks to the WAVES research group at Ghent University for providing access to their capacity based deployment tool and therefore making this research possible.

References

[1] "Base overschreed stralingsnormen na aanslagen," De standaard, 2019.

[2] L. Hardell and C. Sage, "Biological effects from electromagnetic field exposure and public exposure standards," Biomedicine and Pharmacotherapy, vol. 62, no. 2, pp. 104 – 109, 2008.

[3] "What are electromagnetic fields." https://www.who.int/peh-emf/about/WhatisEMF/en/index1.html. Accessed: 15-10-2019.

[4] "Elektromagnetische velden en gezondheid: Uw wegwijzer in het elektromagnetische landschap," Federale overheidsdienst: volksgezondheid, veiligheid van de voedselketen en leefmilieu, vol. 5, 2014.

[5] "Normen zendantennes." https://omgeving.vlaanderen.be/normen-zendantennes. Accessed: 19-03-2020.

[6] E. Commission, "Council recommendation of 12 july 1999 on the limitation of exposure of the general public to electromagnetic fields (0 hz to 300 ghz)," Official Journal of the European Communities, vol. 59, 1999.

[7] D. Plets, W. Joseph, K. Vanhecke, and L. Martens, "Exposure optimization in indoor wireless networks by heuristic network planning," Progress In Electromagnetics Research, vol. 139, pp. 445–478, 01 2013.

[8] M. Deruyck, E. Tanghe, D. Plets, L. Martens, and W. Joseph, "Optimizing lte wireless access networks towards power consumption and electromagnetic exposure of human beings," Computer Networks, vol. 94, 12 2015.

[9] D. Plets, W. Joseph, S. Aerts, K. Vanhecke, G. Vermeeren, and L. Martens, "Prediction and comparison of downlink electric-field and uplink localised sar values for realistic indoor wireless planning," Radiation Protection Dosimetry, vol. 162, no. 4, pp. 487–498, 2014.

[10] D. Plets, W. Joseph, K. Vanhecke, and L. Martens, "Downlink electric-field and uplink sar prediction algorithm in indoor wireless network planner," in The 8th European Conference on Antennas and Propagation (EuCAP 2014), pp. 2457–2461, IEEE, 2014.

[11] S. Kuehn, S. Pfeifer, B. Kochali, and N. Kuster, "Modelling of total exposure in hypothetical 5g mobile networks for varied topologies and user scenarios," Final Report of Project CRR-816, Available on line at: https://tinyurl. com/r6z2gqn, 2019.

[12] D. Plets, W. Joseph, K. Vanhecke, G. Vermeeren, J. Wiart, S. Aerts, N. Varsier, and L. Martens, "Joint minimization of uplink and downlink whole-body exposure dose in indoor wireless networks," BioMed research international, vol. 2015, 2015.

[13] Y. Zeng, Q. Wu, and R. Zhang, "Accessing from the sky: A tutorial on uav communications for 5g and beyond," Proceedings of the IEEE, vol. 107, no. 12, pp. 2327–2375, 2019.

[14] Y. Kawamoto, H. Nishiyama, N. Kato, F. Ono, and R. Miura, "Toward future unmanned aerial vehicle networks: Architecture, resource allocation and field experiments," IEEE Wireless Communications, vol. 26, no. 1, pp. 94–99, 2018.

[15] R. Gangula, O. Esrafilian, D. Gesbert, C. Roux, F. Kaltenberger, and R. Knopp, "Flying rebots: First results on an autonomous uav-based lte relay using open airinterface," in 2018 IEEE 19th International Workshop on Signal Processing Advances in Wireless Communications (SPAWC), pp. 1–5, IEEE, 2018.

[16] M. Deruyck, J. Wyckmans, W. Joseph, and L. Martens, "Designing uav-aided emergency networks for large-scale disaster scenarios," EURASIP Journal on Wireless Communications and Networking, vol. 2018, 12 2018.

[17] G. Castellanos, M. Deruyck, L. Martens, and W. Joseph, "Performance evaluation of direct-link backhaul for uav-aided emergency networks," Sensors, vol. 19, no. 15, p. 3342, 2019.

[18] M. Mozaffari, W. Saad, M. Bennis, Y.-H. Nam, and M. Debbah, "A tutorial on uavs for wireless networks: Applications, challenges, and open problems," IEEE communications surveys & tutorials, vol. 21, no. 3, pp. 2334–2360, 2019.

[19] Q. Wu, L. Liu, and R. Zhang, "Fundamental trade-offs in communication and trajectory design for uav-enabled wireless network," IEEE Wireless Communications, vol. 26, no. 1, pp. 36–44, 2019.

[20] M. Deruyck, A. Marri, S. Mignardi, L. Martens, W. Joseph, and R. Verdone, "Performance evaluation of the dynamic trajectory design for an unmanned aerial base station in a single frequency network," in 2017 IEEE 28th Annual International Symposium on Personal, Indoor, and Mobile Radio Communications (PIMRC), pp. 1–7, IEEE, 2017.

[21] A. V. Savkin and H. Huang, "Deployment of unmanned aerial vehicle base stations for optimal quality of coverage," IEEE Wireless Communications Letters, vol. 8, no. 1, pp. 321–324, 2018.

[22] H. Huang and A. V. Savkin, "A method for optimized deployment of unmanned aerial vehicles for maximum coverage and minimum interference in cellular networks," IEEE Transactions on Industrial Informatics, vol. 15, no. 5, pp. 2638–2647, 2018.

[23] C. T. Cicek, H. Gultekin, B. Tavli, and H. Yanikomeroglu, "Uav base station location optimization for next generation wireless networks: Overview and future research directions," in 2019 1st International Conference on Unmanned Vehicle Systems-Oman (UVS), pp. 1–6, IEEE, 2019.

[24] A. Rizwan, D. Biswas, and V. Ramachandra, "Impact of uav structure on antenna radiation patterns at different frequencies," in 2017 IEEE International Conference on Antenna Innovations & Modern Technologies for Ground, Aircraft and Satellite Applications (iAIM), pp. 1–5, IEEE, 2017.

[25] M. Nosrati, A. Jafargholi, and N. Tavassolian, "A broadband blade dipole antenna for uav applications," in 2016 IEEE International Symposium on Antennas and Propagation (APSURSI), pp. 1777–1778, IEEE, 2016.

[26] M. Nosrati, A. Jafargholi, R. Pazoki, and N. Tavassolian, "Broadband slotted blade dipole antenna for airborne uav applications," IEEE Transactions on Antennas and Propagation, vol. 66, no. 8, pp. 3857–3864, 2018.

[27] B. A. Arand, R. Shamsaee, and B. Yektakhah, "Design and fabrication of a broadband blade monopole antenna operating in 30 mhz–600 mhz frequency band," in 2013 21st Iranian Conference on Electrical Engineering (ICEE), pp. 1–3, IEEE, 2013.

[28] L. Akhoondzadeh-Asl, J. Hill, J.-J. Laurin, and M. Riel, "Novel low profile wideband monopole antenna for avionics applications," IEEE transactions on antennas and propagation, vol. 61, no. 11, pp. 5766–5770, 2013.

[29] S. S. Siddiq, G. Karthikeya, T. Tanjavur, and N. Agnihotri, "Microstrip dual band millimeter-wave antenna array for uav applications," in 2016 21st International Conference on Microwave, Radar and Wireless Communications (MIKON), pp. 1–4, IEEE, 2016.

[30] Y. Zheng, J. Zhou, W. Wang, and M. Chen, "A low-profile broadband circularly polarized antenna array for uav ground-to-air communication," in 2018 IEEE Asia-Pacific Conference

on Antennas and Propagation (APCAP), pp. 219–220, IEEE, 2018.
[31] X. Sun, R. Blázquez-García, A. García-Tejero, J. M. Fernández-González, M. Burgos-García, and M. Sierra-Castañer, "Circular array antenna tor uav-uav communications," in 2017 11th European Conference on Antennas and Propagation (EUCAP), pp. 2025–2028, IEEE, 2017.
[32] I. Singh and V. Tripathi, "Micro strip patch antenna and its applications: a survey," Int. J. Comp. Tech. Appl, vol. 2, no. 5, pp. 1595–1599, 2011.
[33] K. Kashwan, V. Rajeshkumar, T. Gunasekaran, and K. S. Kumar, "Design and characterization of pin fed microstrip patch antennae," in 2011 Eighth International Conference on Fuzzy Systems and Knowledge Discovery (FSKD), vol. 4, pp. 2258–2262, IEEE, 2011.
[34] A. Sudarsan and A. Prabhu, "Design and development of microstrip patch antenna," International Journal of Antennas (JANT) Vol, vol. 3, 2017.